Applied Clay Science 250 (2024) 107291

Contents lists available at ScienceDirect

Applied Clay Science

journal homepage: www.elsevier.com/locate/clay

Research Paper

Reappraisal of red clays in porcelain stoneware production: Compositional and technological characterization

Riccardo Fantini [a], Sonia Conte [b], Alessandro F. Gualtieri [a], Michele Dondi [b], Francesco Colombo [a], Mattia Sisti [a], Chiara Molinari [b], Chiara Zanelli [b], Rossella Arletti [a,*]

[a] Dipartimento di Scienze Chimiche e Geologiche – Università degli Studi di Modena e Reggio Emilia, Via G. Campi 103, Modena I-41125, Italy
[b] Istituto di Scienza, Tecnologia e Sostenibilità per lo Sviluppo dei Materiali Ceramici (CNR- ISSMC), Via Granarolo 64, Faenza (RA) I - 48018, Italy

ARTICLE INFO

Keywords:
iron bearing clays
Porcelain stoneware
Technological properties
Mineralogical and chemical composition

ABSTRACT

The disruption of the supply chain of ball clays from Donetsk basin, Ukraine, has demonstrated that relying on domestic raw materials is strategic and vital for the ceramic tile production. However, the use of local raw materials has in most cases led to the increase in the impurities, namely iron, content of porcelain stoneware batches. A case-study is presented about the Italian tile district located in the Sassuolo area. In this work, we undertook the full characterization of two red clays from local quarries that are iron-rich (~7% Fe_2O_3), thus leading to well-known issues in the ceramic tile production. The features of these samples were compared with those of a German ball clay containing ~3% Fe_2O_3. The complex mineralogical composition of the Val Rossenna varicolored clays and on the Monte Piano marls was unravelled, revealing that they are rich in illite-smectite (I—S) mixed layers and illite, and poor in chlorite, sulfates and organic matter. The effects of a partial substitution in a porcelain stoneware body of classic ball clays with the Italian and German red clays were investigated. The obtained bodies were fully characterized from milling to firing. The amount of the red clays was chosen to best evaluate the effect of iron on the technological properties of semifinished and finished products. The substitution of the classic ball clays with red clays did not introduce unsolvable bottlenecks in ceramic tile production. The addition of the German red clay resulted in a slight increase of the sintering temperature (compared to the benchmark), possibly related to the higher quartz content of this raw material. Conversely, the addition of the Italian red clay induced a reduction of the firing temperature (compared to the benchmark), likely due to the higher content of iron, feldspars and carbonates. The most significant variations concern the color of fired tiles, which results darker (compared to the benchmark) in all the tested bodies, for the presence of pyroxene, hematite, and iron dissolved in the vitreous phase.

1. Introduction

The production of ceramic tiles is growing worldwide and reached ~18.000 million m^2 in 2021 (ACIMAC, 2022). This fact clearly implies a huge demand of raw materials, among which ball clays have been increasingly used, in particular in the production of porcelain stoneware tiles. Such products are manufactured starting from triaxial batches (fluxes, plastic component, skeleton) where clays are close 40% by weight. Until 2022, the ceramic production in Europe, Middle East and northern Africa largely relied on ball clays imported from the Donetsk basin in Ukraine (Fiederling-Kapteinat, 2004, 2005). These clays present peculiar technological features, since they exhibit suitable rheological properties, high plasticity, proper behavior during compaction, easy sinterability, and light color after firing (Dondi et al., 2003; Galos, 2011a; Galos, 2011b; Zanelli et al., 2015). These properties stem from mineralogical composition (kaolinite, illite, random illite-smectite mixed layers (I—S) with a low expandable component and scarce quartz) and grain size distribution. This kind of ball clays is sought after, in particular for the production of large slabs.

The disruption of the supply chain from Ukraine following Russian invasion, with around 4 million tons per year delivered only to EU in 2021 (according to SCREEN, 2023), has caused a shortage of clay in many countries. This caused a domino effect with a rush to find out alternative sources of ceramic clays. The secure access to mineral resources turned to be a competitive factor among tile manufacturers and the dependence on few sources proved to be critical for the supply risk

* Corresponding author.
E-mail address: rossella.arletti@unimore.it (R. Arletti).

https://doi.org/10.1016/j.clay.2024.107291
Received 10 November 2023; Received in revised form 21 December 2023; Accepted 6 February 2024
Available online 17 February 2024

(Fahimnia et al., 2015). The demand of highly plastic and white-firing clays is increasing because of the spread of ceramic slab production that needs top quality raw materials. The import reliance of the European ceramic tile industries is high for both plastic and non-plastic raw materials, and attained in the latest years a value close to 80% for ball clays used by the Italian ceramic district (Dondi et al., 2021).

The ceramic sector is focusing on resource efficiency and this interest has been growing continuously in relation to the current need to improve sustainability. In this regard, circular economy practices push the introduction of waste into the production system (Zanelli et al., 2021). Unfortunately, this cannot always be fulfilled for every raw material. Thus, the use of local raw materials should be promoted in order to reduce energy consumption for transportation and related CO_2 emissions (Dondi, 1999; Timillini et al., 1999; Dondi et al., 2019). Although Italy has a wide range of clay suppliers (Germany, Turkey, Romania, Serbia, Spain, Portugal, France, United Kingdom, etc.) it may be necessary to resume using local raw materials for porcelain stoneware tiles, regardless of their iron content.

We take the Italian ceramic district, located in the Sassuolo area, as a case study. In the 1950–1980 period, its production was based on local red clays only, before converting first to light-colored stoneware and eventually to porcelain stoneware (Dondi, 1999) which now represents ~90% of the tiles output. Expanding the available sources of raw materials is essential to mitigate the supply risk and, in consequence of recent shortage, local clays have returned to use in very small percentages in porcelain stoneware, even if they miss some of the desired features. Although there is a large body of literature on clays from northern Apennines, mineralogical data are generally qualitative and the ceramic characterization referred to technologies that are no longer in use (Dondi, 1999). Therefore, to understand in depth their suitability for porcelain stoneware production, a detailed characterization is needed, and is one of the aims of this work.

A comprehensive characterization of two clays from quarries located near the Sassuolo ceramic district and on a German red clay for comparison is provided: quantitative chemical and phase analysis, plasticity evaluation and behavior in the different steps of the production cycle of ceramic tiles (from milling to firing) are here presented. The goal of the present work is to assess the effect of Fe-rich clay materials into a standard batch for the production of porcelain stoneware tiles. The amount of the red clay was stressed beyond the usual addition to the batch nowadays (≤3 wt%) in order to shed light on the role of iron on technological behavior and color of the final product. The German red clay was selected as a reference material because it is a conventional ball clay containing iron. This means that is compatible to sources already employed in the production of porcelain stoneware tiles in terms of mineralogical composition, but is richer in iron. Actually, the most widespread and commercially available iron-rich ball clays come from Westerwald (Germany), which, moreover, is the second largest supplier of clays for the Italian ceramic tile industry. The comparison among the behavior of the batches produced with the Italian red clay and with a red ball clay will help in distinguishing between the effect due to the presence of iron and to the different.

mineralogical composition.

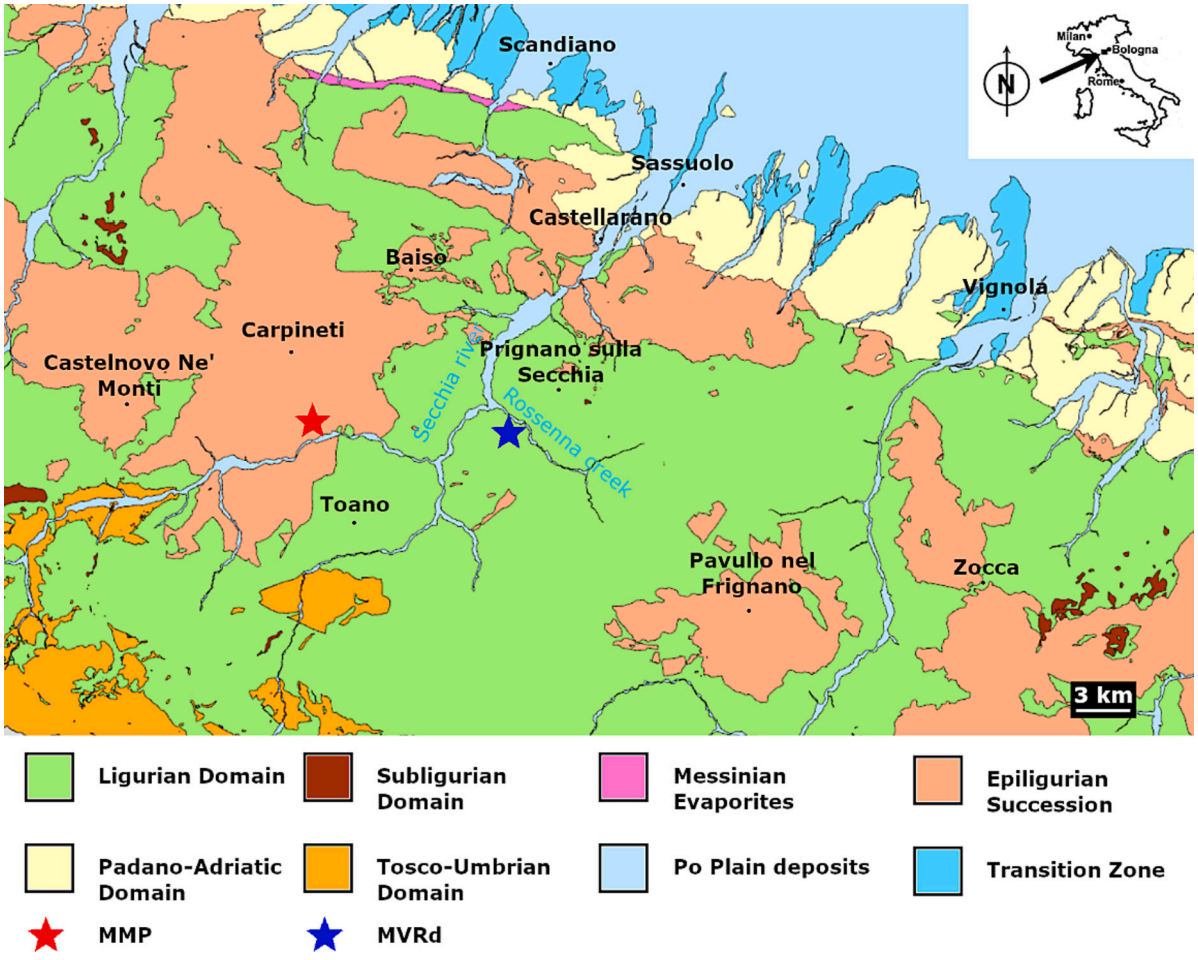

Fig. 1. Geological sketch map of the Sassuolo district. (Modified after Geoportale 3D Emilia Romagna- Geologia di Sintesi https://mappe.regione.emilia-romagna.it/#share=g-bb847447293f89ef6d6a40e233fd5852&share=g-ef692be2ca990e4d1366adf7ac02a5e2).

2. Materials and methods

2.1. Materials and geological setting

Three red-firing clays were taken into account: MVRd (Val Rossenna varicolored shale), MMP (Marne di Monte Piano Formation) and GBC (German ball clay rather rich in iron). All the clay samples used for this study are commercial samples deriving from quarries.

Val Rossenna varicolored shale (MVRd) was extracted from the Caselette quarry, a classic source for red bodies (Bertolani et al., 1982; Vignudini and Venturi, 1996; Dondi, 1999). This unit belongs to the Rio Cargnone Complex (Ligurian Domain, Fig. 1), i.e. a chaotic assemblage of sedimentary origin (Upper Paleocene-Middle Eocene) interpreted (Bettelli et al., 1989a, 1989b) as the result of the accumulation of large mass landslides (mudslides and debris) in the sub-sea environment. The sample object of this study derives from inclusions of varicoloured shales present in the complex, which strongly resemble the varicoloured shales of Cassio (i.e., MVRd). They are lithologically very heterogeneous, but mainly constituted by the rhythmic alternation of red, grey, greenish and blackish clays with very thin stratification with frequent intercalations of arenaceous pelagic turbidites, light grey and greenish siliceous calcilutites, whitish marly calcilutites, variable grain sandstones and breccias and coarse sandstone. The depositional environment can be identified as a deep submarine plain located near or below the CCD (Calcite Compensation Depth, depth of marine waters below which the speed of dissolution of calcite exceeds that of accumulation, from the maximum value of about 5000 m) with distal turbidite inputs from many different sources.

Monte Piano Formation (MMP): The material was extracted from the Sopra Vigne quarry in the main clay mining district in Northern Apennines (Bertolani et al., 1982; Capelli and Bertolani, 1991; Dondi, 1999). This formation consists of argillites, marly clays and marls of red, pinkish, light grey and green-grey color with rare thin layers of whitish arenaceous turbidites, very dark siltstones and grey-green marly limestones (Bettelli et al., 2002). They occur in thin layers, often poorly defined, of blackish siltstones, fine resedimented whitish sandstone and, more rarely, marly and green-grey calcilutites are present as well. The stratification is rarely observable in an undeformed layer at the scale of the outcrop and is often obliterated by complex plicative and shear deformation structures. Most of these structures suggest formation during the initial stages of lithification in this clayey lithotypes, possibly reflecting deformations linked to slumping phenomena The sedimentation environment refers to a deep basin characterized by the settling of pelagic shales and to the influx of diluted turbidity currents with exclusive resedimentation of fine and very fine terrigenous material. The marls date back to the Eocene era, more precisely between the Lutetian and the Priabonian (Bettelli et al., 2002), and occurs within the Epiligurian domain (Fig. 1).

German red clay (GBC) came from the Westerwald area in Germany. The clay deposits are of fluvial-lacustrine environment and derive from the alteration and erosion of greywacke, shales and Devonian quartzites (Petrick et al., 2011; Bornhöft and Kleeberg, 2012). These deposits date back to Eocene-Oligocene.

2.2. Characterization of red clays

Chemical characterization of the clays was carried out by wavelength-dispersive X-ray fluorescence spectrometry (XRF-WDS, Philips PW1480, Eindhoven, the Netherlands) by applying the methods proposed by (Franzini et al., 1975; Leoni and Saitta, 1976). Measurements were performed on pressed powder pellets obtained using calcined powder in order to avoid pellet damage upon hydration. Analyses are considered accurate within 2–5 wt% for major elements (Na, Mg, Al, Si, P, K, Ca, Ti, Mn, Fe), and better than 10 wt% for trace elements (Ni, Co, Cr, V, Ce, Nd, Ba, La, Zr, Y, Sr, Rb, Pb, As, Zn, Cu, Cd, S, Cl).

For the evaluation of organic carbon, elemental analyses were performed using a Thermo-Fisher CHNS FLASH 2000 analyzer. The bulk clays, after the removal of carbonates via HCl attack, were brought at 1800 °C with a "FLASH" dynamic combustion. After the reduction, the elementary gases released by the decomposition were analyzed in a GC (gas-chromatograph) comprising a chromatographic column and a sensitive TCD detector.

Thermogravimetric (TGA) and thermo-differential (DTA) analyses were performed (Seiko SSC 5200 thermal analyzer, 25–1050 °C range, heating rate 10 °C/min) in order to obtain information of the hydrated phases present in the bulk clays and to evaluate the loss on ignition (LOI).

Qualitative and quantitative mineralogical analyses were performed on bulk both clays and fired ceramics. X-Ray powder diffraction patterns were collected using a θ–θ Bragg-Brentano PANalytical 'XPert Pro Diffractometer (Cu Kα radiation) equipped with a real time multiple strip (RTMS) detector. Samples were ground using an agate mortar and the powder was mixed with 10 wt% of corundum Al_2O_3 as an internal standard. To avoid preferred orientation side loading of the sample powder was chosen. Data were collected in the angular range 3–110°2θ using step scan of 0.0167°2θ and a counting rate of 12 s/step. A ½° divergence slit was used and 0.04° Soller slits. The XRPD patterns were analyzed using the X-Pert High Score Plus suite (Degen et al., 2014).

For the qualitative evaluation of the clay minerals present in the samples, three specimens for each red clay were prepared by suspending 2 g of bulk clay in 50 ml of deionized water with the addition of one drop of NH_4OH. Then the grain size fraction <2 μm was concentrated by Stokes' law, and settled on a glass slide to obtain a basal-oriented powder and enhance the (00*l*) reflections. X-ray powder diffraction pattern were then collected in the theta range 3–14°2θ: 1) in air; 2) after thermal treatment at 550 °C for 30 min; 3) after ethylene glycol solvation.

Quantitative phase analyses (QPA) of all the considered samples were obtained after Rietveld - RIR refinement (Gualtieri, 2000; Gualtieri et al., 2019) performed using the Profex version 5.0.2 software (Doebelin and Kleeberg, 2015). Structural model for the refinements were taken from the Profex database.

In addition, the ferromagnetic fraction of the Italian clays was investigated to focus on the Fe-bearing phases. After quartering, a known aliquot of bulk, unprocessed, MVRd and MMP was suspended in water and sonicated for 10 min. Then, the suspension was passed through a column equipped with six strong neodymium magnets to retain the ferromagnetic portion. The process was repeated three time on the same suspension, and the total amount of ferromagnetic fraction was finally quantified. The fraction with grain size above 50 μm was further separated from the non-magnetic portion via sedimentation. This coarse fraction was sampled thanks to an optical stereoscope, focusing on particles with metallic luster, since some Fe-bearing particles are not ferromagnetic (e.g. pyrite). The ferromagnetic and the selected coarse fractions were then analyzed by SEM for morphological and chemical analysis. The employed instrument is a Jeol JSM-6010PLUS/LA SEM microscope equipped with and Energy Dispersive X-ray (EDX) spectrometer (Oxford INCA-350). The operating voltage was 20 keV, and the working distance 10 mm.

To evaluate the plasticity of the tested bulk clays, Atterberg limits (PL Plastic Limit, LL Liquid Limit, PI = LL-PL plastic index) were determined by the ISO/TS 17892–12:2004 standard.

2.3. Technological characterization of batches

On the basis of the results of the three clays mineralogical composition (see Section 3.3 and Table 3), two of them were tested in substitution of the common material employed in the industrial production (Ukranian ball clay). Specifically, the German ball clay and MMP sample were selected, since the low amount of kaolinite of MVRd can compromise a good degree of mullitisation of the ceramic body, leading to the

presence of a small quantity of skeleton at high temperatures, with possible repercussions on the stability of the body (Conte et al., 2023).

Five different batches were designed: a benchmark named B0, representing a classical industrial formulation for porcelain stoneware, and four batches containing two different amounts of red clay (20 or 35 wt% of GBC; 10 or 20 wt% of MMP). Ball clays 1 and 2 are from Ukraine, feldspars from Turkey, and quartz sand from Italy. The addition of red clay has been maximized to have a rather high iron content, so as to be able to evaluate its effect on technological behavior, but without straying too far from the compositional field of porcelain stoneware. The designed formulations and their calculated chemical compositions are reported in Table 1.

The batches so realized underwent the simulation of the industrial tile-making process at the laboratory scale. All the raw materials were ball milled in a planetary mill for 25 min: 40 wt% water (by weight of the slip) and 0.3 wt% deflocculant (sodium tripolyphosphate) by weight of dry batch for B0, GBC20 and GBC35, while for MMP10 and MMP20 0.6 wt% deflocculant was used, since the MMP clay tends to worsen the slip rheology. The slips were oven dried, de-agglomerated (hammer mill with grid of 750 μm) and manually granulated (sieve 2 mm, moisture ~8 wt%). Powders were compacted with a hydraulic press (40 MPa) into 50 × 5 mm pellets (diameter x height), then dried in electric oven (105 °C overnight).

The technological behavior of unfired samples was appraised through the determination of the following characteristics: particle size distribution by X-ray monitoring of gravity sedimentation (ASTMC958); powder moisture (ASTM C324); green and dry bulk density (weight/volume ratio); springback after pressing (i. e., 100(*D*p - *D*m)/*D*m where *D*p is the diameter of the pressed disk and *D*m is the diameter of the mold).

Powder compacts were fast fired in an electric kiln (ER15; Nannetti, Faenza, Italy) at different maximum temperature (Tmax). Specifically, a first firing was conduced for all the bodies at 1200 °C, then, based on the measured water absorption, WA, and bulk density, DB, two different set of T°C were established in order follow the evolution of technological properties from an incomplete sintering to overfiring conditions. By this way, B0, GBC20, GBC35 were fired at T_{max} = 1160, 1180, 1200, 1220 and 1240 °C, while batches MMP10 and MMP20 were fired at T_{max} = 1140, 1160, 1180, 1200 e 1220 °C. The thermal cycle consisted in a 60 min cold-to-cold cycle and 5 min of dwell time at T_{max}. Linear firing shrinkage (i.e., (i.e., 100(D_m - D_f)/D_m where D_f is the diameter of the fired disk and D_m is the diameter of the mold), water absorption, bulk density and open porosity (ASTM C373) were determined. CIE-Lab colorimetry (ISO 10545-16, MSXP-4000; Hunterlab, Reston, VA, USA) of sintered tiles was also performed to get L^*, a^*, and b^* coordinates.

The phase composition of tiles fired at the temperature of maximum densification was obtained by Rietveld-RIR refinement, following the protocol employed for the raw material characterization (see section 2.2).

3. Results and discussion

3.1. Chemical composition of red clays

The chemical composition of the clays coming from near the Sassuolo district are comparable (Table 2). The varicolored shale (MVRd) is richer in silica and alumina, while the Monte Piano clay has more calcium and loss on ignition; the remaining oxides are in rather similar amounts. The German red clay is poorer of alkali and alkaline earths but richer in silica with respect to Apenninic raw materials. The iron is

Table 1
Formulations of porcelain stoneware batches, their chemical and mineralogical composition (wt%) (calculated on the basis of chemistry and mineralogy of raw materials, see results section). In the mineralogical composition, accessory minerals refers to all other phases not included in the list.

		B0	GBC20	GBC35	MMP10	MMP20
Plastic component	Ball clay 1	20	10	2.5	15	10
	Ball clay 2	20	10	2.5	15	10
	GBC clay		20	35		
	MMP clay				10	20
Fluxes	Feldspars	45	45	45	45	45
Filler	Quartz sand	15	15	15	15	15
Total		100	100	100	100	100
Chemical composition						
SiO_2		71.25	72.42	73.31	70.83	70.42
TiO_2		0.64	0.67	0.68	0.61	0.57
Al_2O_3		20.10	18.62	17.51	19.16	18.23
Fe_2O_3		0.66	1.03	1.30	1.35	2.04
MgO		0.58	0.61	0.63	0.90	1.22
CaO		0.53	0.48	0.45	0.65	0.78
Na_2O		4.88	4.81	4.75	5.00	5.13
K_2O		1.36	1.36	1.36	1.49	1.62
Total		100	100	100	100	100
Mineralogical composition						
kaolinite		19.8	14.1	9.9	16.1	12.5
mica (illite/muscovite)		10.2	7.2	5.0	9.4	8.5
mixed layer clay		0.0	2.5	4.4	3.4	6.8
Fe-oxides		0.5	0.5	0.5	0.5	0.5
quartz		25.8	30.3	33.7	25.4	25.1
plagioclase		40.4	40.6	40.8	40.9	41.4
K-feldspar (orthoclase)		1.5	2.8	3.8	2.2	3.0
calcite		0.0	0.1	0.1	0.2	0.3
dolomite		0.0	0.0	0.0	0.1	0.2
accessory minerals		1.8	1.8	1.8	1.7	1.6
TOTAL		100	100	100	100	100
Sum Plastic phases		30.03	23.87	19.25	28.91	27.79
Sum Feldspars		41.8	43.4	44.6	43.1	44.4

Table 2
Chemical composition for major, minor and trace elements of red clays. (LOI = lost on ignition; TOC = total organic carbon).

Wt%	GBC	MVRd	MMP
	wt%		
SiO_2	62.22	56.20	53.81
TiO_2	1.16	0.83	0.74
Al_2O_3	18.43	18.89	16.82
Fe_2O_3	2.66	7.37	7.10
MnO	0.01	0.15	0.18
MgO	0.60	3.12	3.28
CaO	0.13	0.51	1.43
Na_2O	0.16	1.56	1.56
K_2O	1.81	3.23	2.97
P_2O_5	0.05	0.12	0.11
TOC	0.15	0.14	0.15
LOI	12.76	8.05	12.00
	ppm		
Ni	45	68	65
Co	13	36	28
Cr	139	105	90
V	152	159	142
Ce	125	95	65
Nd	45	30	34
Ba	243	309	420
La	65	39	35
Zr	347	246	196
Y	35	34	27
Sr	64	164	193
Rb	98	180	154
Pb	31	27	22
As	8	12	8
Zn	30	117	109
Cu	<30	81	57
S	<30	36	171
Cl	<40	<40	<40

remarkably different with respect to the Italian clays: GBC has a Fe_2O_3 content around 2.7 wt%, at variance of MVRd and MMP where iron oxide is around 7 wt%. It is worth noting the absence of organic matter, as testified by the absence of organic carbon, and the low amount of sulfur, clearly excluding a significant quantity of sulfur-bearing phases. These considerations are particularly important, since the presence of sulfides, sulfates, and of organic matter can represent a crucial issue for the use of these raw materials in ceramic production. In fact, organic matter in clays can cause undesired effects in tiles properties, it can change the color, reduce mechanical strength, increase fire loss (due to its volatility), and increase the firing costs. On the other hands, the presence of sulfides can lead to unwanted gas emission during firing.

3.2. Qualitative mineralogical composition of red clays

The identification of clay minerals was done on the basis of both X-Ray powder diffraction patterns (oriented samples in air, after thermal treatment and ethylene glycol saturation, Fig. 2) and thermal analyses.

The clays MVRd and MPP are quite similar but different from GBC (Fig. 2). All patterns collected in air show peaks at 12.3°2θ (~7 Å), 8.8°2θ (~10 Å), a broad one centered at 7°2θ (~12.5 Å), and a small peak at ~6°2θ (~ 14 Å), more marked in MMP. In both the Italian samples, we can hypothesize from the shape of the peak at 10 Å that illite should prevail on micas. The complete disappearance of the peak at ~7 Å after heating indicates it pertains to kaolinite only, excluding thus the presence of chlorite, despite it was always found in the literature (Bertolani et al., 1982; Fiori and Guarini, 1990; Capelli and Bertolani, 1991; Vignudini and Venturi, 1996). A pattern collected on a different oriented section treated at lower temperature (500 °C, data not reported) confirmed the disappearance of the peak. Nevertheless, after the thermal treatment, the intensity of the peak at ~12.5 Å strongly decreased, evidencing the presence of a weak peak at ~14 Å that can be indexed as the (001) reflection of chlorite. In fact, even if the drop of 7 Å reflection at high temperature seems to rule out the presence of chlorite (002) reflection, the phase can be present in low amount. From the plot reported in Fig. 3 it is evidenced how the intensity ratio of (001) and (002) chlorite reflections are strongly influenced by Mg and Fe distribution (Moore and Reynolds Jr, 1989). Indeed, considering a structural model in which all the octahedral sites of TOT layer are occupied by iron and all the interlayer octahedral sites are occupied by Mg (Fig. 3), (002) reflection show a weaker intensity if compared to (001). The presence of small amount of chlorite, with iron present mainly in TOT layers, can thus justify the presence of only (001) reflection, being (002) too weak to be observed. Moreover, Moore and Reynolds Jr (1989) also highlights how the (002) intensity of chlorite is much weakened by the 550 °C thermal treatment, corroborating our interpretation.

The changes to low-angle peaks observed after the thermal treatment suggest the occurrence of illite/smectite (I—S) mixed layers and/or smectite, which both collapse on the (001) peak of illite (~10 Å) upon heating. This is corroborated by the ethylene glycol saturation test, as the shift of the broad peak from ~12.5 Å to the 10–14 Å interval can be ascribed to I/S interstratified terms, likely with illite prevalent over smectite, even though a small fraction of true smectite cannot be excluded.

The German ball clay contains mainly kaolinite (7 Å peak disappearing over 550 °C) and illite (asymmetric peak at 10 Å). The absence of any diffraction signal at 14 Å and the disappearance of the 7 Å peak after heating exclude the presence of chlorite. The ethylene glycol saturation slightly modifies the 10 Å peak (more symmetric) and let a broad band to appear at ~13.2 Å (I—S expandable phases, with illite domains strongly prevailing on smectite ones). This mineralogical composition corresponds to a previous investigation on Westerwald clays (Petrick et al., 2011).

In terms of non-clay mineral phases, MVRd, MMP, and GBC are quite similar. From qualitative XRPD, the main non-clay phases are quartz, k-feldspar, plagioclase, with minor calcite, dolomite, anatase, rutile,

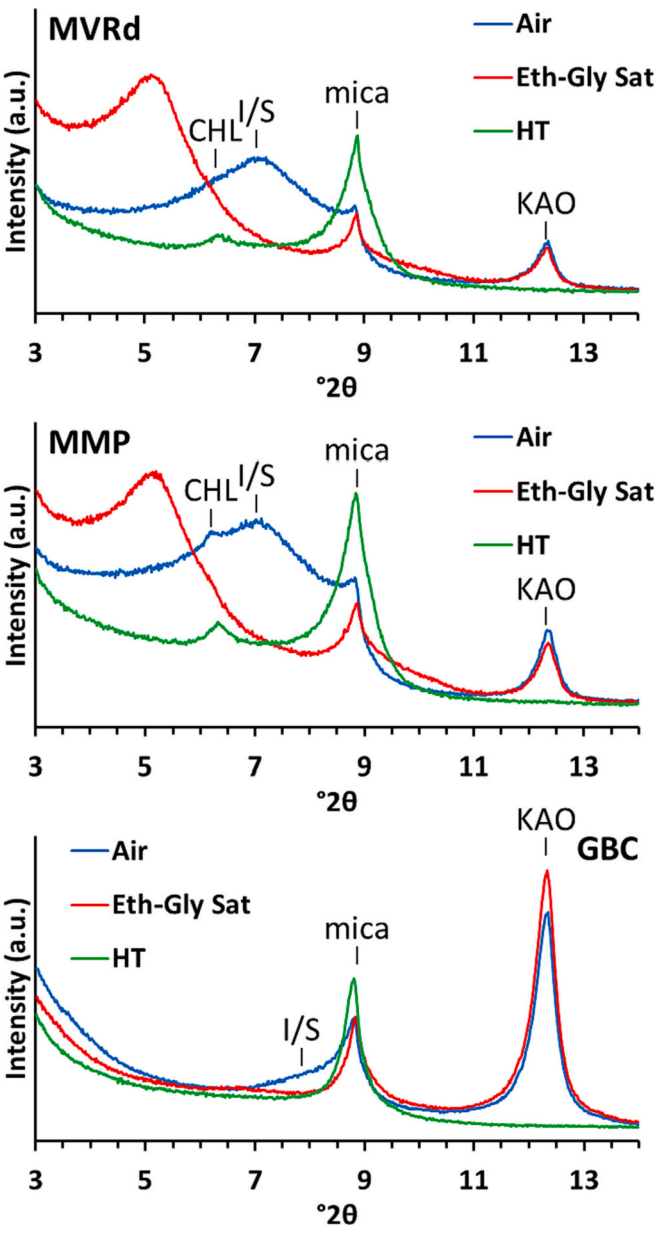

Fig. 2. Diffraction patterns collected on oriented samples (MVRd, MMP, GBC) in air (blue), after thermal treatment (green) and on ethylene glycol saturated samples (red). Markers are KAO: kaolinite and chlorite; mica: illite/muscovite; I/S: I/S mixed layers; CHL: chlorite. (For interpretation of the references to color in this figure legend, the reader is referred to the web version of this article.)

hematite and goethite. Concerning the Fe-bearing phases, sulfides and sulfates were not detected by XRD, even if, at least for MVRd and MMP, their presence is well known and also evident during field survey. In this concern, the SEM morphological and chemical analyses on enriched ferromagnetic and coarse fractions of MVRd and MMP confirmed the presence of at least hematite (lamellar iron oxide), pyrite (octahedral iron sulfides), metallic copper, and iron (possibly cosmic dust). Some examples of particles are reported in Fig. S1 and S2 of supplementary materials. It must be highlighted that the ferromagnetic fractions account for no >0.3 wt% in MVRd and MMP. Also, particles with metallic luster (e.g. sulfides) are only a minor part of the coarsest fraction. The very low amount of sulfides detected may derive from the selective extraction of quarry material. Sulfides (especially pyrite and marcasite) are indeed generally concentrated into specific horizons (e.g. coarser

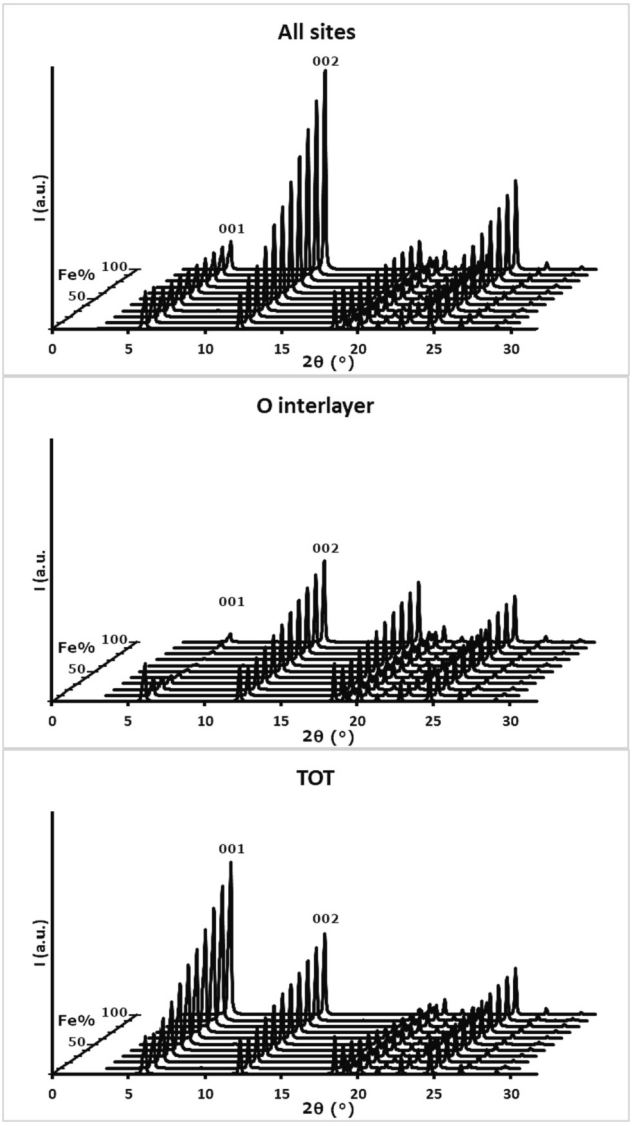

Fig. 3. Chlorite XRPD pattern calculated changing the Fe/Mg ratio in all sites (top), in the interlayer octahedral site (middle) and in the TOT octahedral site (bottom). In the models of figures (top) and (middle), the remaining sites, i.e. TOT and O respectively, are totally occupied by Mg.

turbidites and hardgrounds) which are discarded during operations. It is plausible that the commercial samples of bulk clay here employed, underwent such kind of operations.

3.3. Quantitative mineralogical composition of red clays: Rietveld data

The quantitative mineralogical analyses obtained by Rietveld method are reported in Table 3. The two Italian clays show higher amount of expandable phases (26.2% and 34.0% for MVRd and MMP, respectively) compared to the German sample (12.7%) which, on the contrary, exhibits the highest amount of kaolinite (19% vs. 5.1% and 10.7%). The amount of illite is more marked in the Italian clays (24.4% and 17.1% for MVRd and MMP, respectively) with respect to the German one (10.5 wt%). Traces of chlorite were detected only in the Italian samples.

Regarding the non-clay phases, in all the samples quartz and feldspar (both plagioclase and K-feldspar) are present, with the higher amount of quartz found in the German sample. Carbonates are present (calcite in GBC and calcite and dolomite for MMP) with the exception of MVRd.

Table 3
Quantitative mineralogical compositions of the three clays obtained by Rietveld-RIR analysis.

Samples		GBC	MVRd	MMP
Goodness-of-fit statistics	R_{wp}	6.31	5.35	5.40
	R_{exp}	4.44	3.86	3.67
	χ^2	2.02	1.92	2.17
mineral		wt%		
kaolinite		19.0(3)	5.1(2)	10.7(4)
mica (illite/muscovite)		10.5(2)	24.4(5)	17.1(7)
I/S Mixed Layers		12.7(4)	26.2(7)	34.0(7)
chlorite		–	0.3(1)	0.3(1)
quartz		44.5(2)	21.4(2)	18.3(2)
Plagioclase (albite)		3.8(2)	9.4(2)	7.9(2)
K-Feldspar (orthoclase)		6.7(3)	9.6(3)	7.5(3)
calcite		0.3(1)	–	1.7(1)
dolomite		–	–	1.1(1)
anatase		–	1.0(1)	0.8(1)
rutile		1.4(1)	0.3(1)	≤0.1
hematite		1.0(1)	2.0(1)	0.6(1)
goethite		–	0.3(1)	–

Ti oxides (anatase, rutile) and Fe oxides and oxyhydroxides (hematite, goethite) are present in low amounts in all the samples, with the higher values referred to MVRd. Such a low amount of crystalline Fe compounds quantified by Rietveld refinement does not match the total iron oxide percentage in the clays, as observed in a previous study (Petrick et al., 2011).

3.4. Thermogravimetric analyses and comparison with quantitative data

The data relative to thermal analyses of the three samples are reported in Fig. 4. The general trend of the TG curves relative to GBC and MVRd are quite similar: a quite steep loss is observed below 200 °C, then a plateau is observed up to 450 °C. A further loss around 640 °C is observed for MMP sample as a rather marked signal, while it is present as a weak peak in the DTG curve of MVRd.

Generally, for clays, the weight loss between 80 and 200 °C is ascribed to smectites and mixed layer-clays dehydration (humidity and interlayer water). The losses below 200 °C correspond to: 3.7 wt% for GBC, 3.3 wt% for MVRd, 4.4 wt% for MMP corresponding to ~27, 25 and 33% of I/S phase. The value is consistent with the XRPD analyses for the two Italian clays but overestimated for GBC samples. These discrepancies can be ascribed to the presence of different degrees of humidity in the samples (as testified by the presence of a double signal in MVRd and MMP samples), in fact humidity losses occur below 100 °C and hardly stand out from structural water. Possible heterogeneities in the sample should be taken into account, as well.

The weight loss between 400 and 600 °C can be referred to the dihydroxylation of mainly illite/mica and kaolinite, and other clay minerals. Generally, when only kaolinite is involved in the reaction, the peak is sharp and the DTG curve appears symmetric. On the contrary, when interlaminate phases are present, the peak is strongly asymmetric, (as reported for MVRd and MMP samples). The losses observed in this temperature range are: 3.7 wt% for GBC and 3 wt% for both the Italian clays. The calculated structural water weight losses deriving from the amount of kaolinite determined by QPA should be 2.7 wt%, 0.7 wt%, 1 wt% for GBC, MVRd and MMP, clearly indicating that in this temperature range other dihydroxylation reactions, involving the other clay minerals, occurs. The loss centered at 640 °C, observed in MMP could be ascribable to decarbonation of calcite and dolomite. Considering a weight loss of 1.26 wt%, it is possible to calculate a content of carbonates of 2.9 wt%, perfectly consistent with the values obtained from quantitative phase analyses (the temperature range considered comprises the decarbonation of both calcite and dolomite). Small losses are observable even for the other two samples: for MVRd a small peak in the DTG peaks is observable, for GBC only a weak shoulder accompanying the dihydroxylation reaction can be detected. From the quantification of

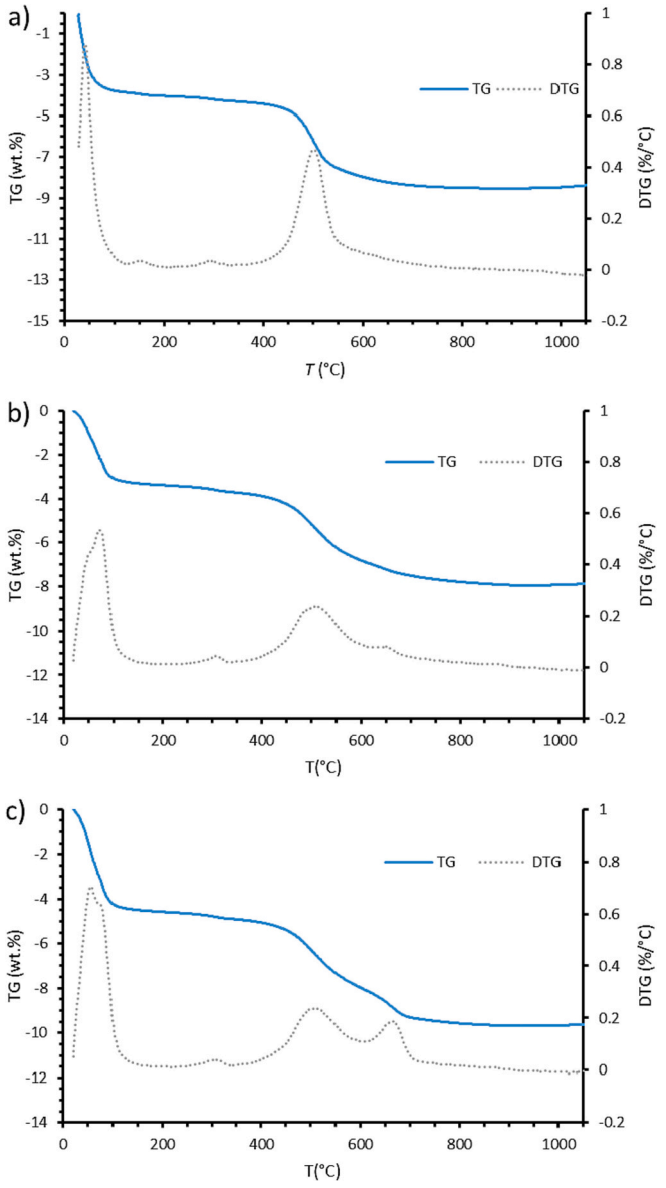

Fig. 4. TG and DTG curves for GBC (a), MVRd (b)and MMP(c) samples.

weight losses observable in the temperature range 550–670 °C, the amount of carbonates should be 0.3% for GBC and 0.4% for MVRd, respectively. This data is consistent with the QPA analysis for the German ball clay, on the contrary, carbonates were not detected in the MVRd sample, this could probably indicate a certain degree of heterogeneity in the material.

All the samples investigated show a very small weight loss from 270 and 350 °C (0.2 wt%), that could be referred to mixed hydroxides. From XRPD analysis, goethite was detected only in MVRd sample, nevertheless it is well known that clays can contain a certain amount of amorphous Fe oxides and hydroxides. As a whole all the samples, on the basis of the thermal analyses, seems to contain about 2% of hydroxides, accounting for both crystalline and amorphous phases. It is worth noting that recognizing 1–2 wt% of amorphous phase exploiting Rietveld refinement is extremely challenging, since it would correspond to an overestimation of the internal standard (α-Al_2O_3, corundum) from 10.0 to 10.2 wt%, which is in the order of magnitude of the error. As a whole, the amount of Fe_2O_3 estimated from QPA and thermal analyses for crystalline and amorphous Fe oxides and hydroxides perfectly matches with chemical data only for German sample (3% -QPA + TG- vs 2.66%-XRF). Chemical analyses of Italian samples show higher levels of Fe_2O_3, with respect to the amount deduced from QPA + TG considering iron oxides and hydroxides (amorphous and crystalline). This could be explained by the presence of high amount of iron in the interlaminated phases and in the illite layers. (Bertolani et al., 1982; Fiori and Guarini, 1990; Capelli and Bertolani, 1991; Vignudini and Venturi, 1996).

3.5. Plasticity of red clays

Atterberg limits are reported in Table 4 and let to classify all the three raw materials as plastic clays, since PI is between 15 and 40 (Polidori and Gori, 2005). Both Apenninic clays are distinctly more plastic than the German ball clay, as expected by their mineralogical composition, clearly richer in expandable clay minerals. The values of MVRd match with literature data on Val Rossenna shales (Dondi, 1999). In contrast, those of MMP are similar to previous studies only for the plastic limit, as the liquid limit (and consequently the plasticity index) are lower than expectable for Monte Piano clays (Dondi, 1999). This could be attributed to the variation in sample sources from different levels within the quarry, where the composition of the extracted material may have changed over the years. It is well established that these quarries exhibit a high degree of heterogeneity. The samples analyzed here accurately represent the currently quarried levels."

3.6. Technological properties of porcelain stoneware tiles: Semifinished products

Particle size distribution of slips is crucial for assessing the outcome of the wet grinding process. All the samples show similar curves (Table 5 and Fig. 5) that fall in the range accepted in the industrial practice. However, it is evident that batches containing GBC have slightly coarser grain sizes compared to the others. Specifically, B0, MMP10 and MMP20 have a median particle diameter (d_{50}) of 3.7 μm versus a d_{50} between 4.3 and 4.7 μm found for GBC-bearing slips. This can be due to the occurrence of more hard minerals, such as quartz, in the German clay. This also means that the presence of MMPs from 10% to 20% did not significantly change the slip rheology, once the amount of deflocculant was correctly increased, since the particle size curves are practically superimposed on the benchmark.

The technological properties of unfired samples are summarized in Table 5. The substitution of highly plastic ball clays with red clays did modify to some extent the properties of the semi-finished products. It can be observed that the introduction of GBC slightly increased the springback with respect to the benchmark. On the contrary, the springback decreased after addition of MMP. This behavior is due to the plasticity (higher for MMP and lower for GBC) and mineralogical composition (more expandable clay minerals in MMP).

Considering the powder compressibility, expressed by the green bulk density, MMP-bearing bodies are denser than the benchmark, while the GBC-bearing samples are less dense than B0. Once again, this is an effect linked to plasticity: using a less plastic clay (like GBC) brings about a lower powder compressibility. Data of dry bulk density are strictly consistent with those observed for green samples.

Overall, all the values obtained for the technological properties of unfired products are in the range usually accepted in the industrial practice (Zanelli et al., 2018, Zanelli et al., 2019; Conte et al., 2022). Thus, we can conclude that no important bottleneck in the production

Table 4
Atterberg Liquid Limit, Plastic limit and index of plasticity for the analyzed samples.

Sample	Plastic limit	Liquid limit	Plasticity Index
GBC	21.0	38.7	17.7
MVRd	30.8	51.9	21.1
MMP	31.3	56.2	24.9

Table 5
Technological properties of unfired products.

	Property	Median particle diameter	Springback	Green bulk density	Moisture	Dry bulk density
	unit	μm	cm/m	g/cm^3	% wt.	g/cm^3
B0	mean	3.7	0.49	2.153	7.79	2.015
	std. dev.	–	0.05	0.010	0.06	0.006
GBC20	mean	4.3	0.53	2.043	7.66	1.912
	std. dev.	–	0.02	0.002	0.04	0.002
GBC35	mean	4.7	0.58	1.977	7.56	1.850
	std. dev.	–	0.02	0.012	0.05	0.011
MMP10	mean	3.7	0.43	2.180	7.83	2.035
	std. dev.	–	0.01	0.018	0.07	0.006
MMP20	mean	3.7	0.42	2.162	7.63	2.024
	std. dev.	–	0.01	0.006	0.16	0.006

cycles was observed.

3.7. Technological properties of the fired products

Technological properties determined after firing at different temperature are reported in table S1, while that determined at the maximum densification temperature in Table 6 and Fig. 6.

The gresification curves of all the batches are compared in Fig. 6, contrasting water absorption and bulk density at different maximum temperatures. Concerning water absorption (WA), MMP10 and MMP20 show low WA levels at the lowest investigated temperatures. Indeed, they reach the WA threshold prescribed for porcelain stoneware (BIa group, ≤0.5 wt%, ISO13006 and ISO/DIS 5644) at lower temperatures with respect to the other samples: 1160 °C for MMP20 and 1180 °C for MMP10°C versus 1200 °C for B0 and 1220 °C for both GBCs. The temperature of maximum bulk density (BD) perfectly matches that of water absorption <0.5%, indicating the appropriate firing temperature for each batch. It is worth noting that the BD trends are different for the various batches. Those containing the Italian red clay exhibit a marked decrease of bulk density after the achievement of the maximum densification. This effect is more severe for MMP20, which contains the highest amount of local clay.

Overall, the data of the BD and WA indicate a narrow range of temperature characterized by a good degree of densification and stability for the red clay bearing batches. It is possible to conclude that the gresification temperature (i.e., the temperature corresponding to a bulk density ~ 2.3–2.4 g/cm^3 and water absorption ≤0.5%) is lower for the bodies containing MMP clays, especially for MMP20 that has 40 °C less than the benchmark. The opposite is observed for GBC-bearing samples, showing a gresification temperature 20 °C higher than B0. This is due to the different mineralogical composition of the clays, richer in refractory

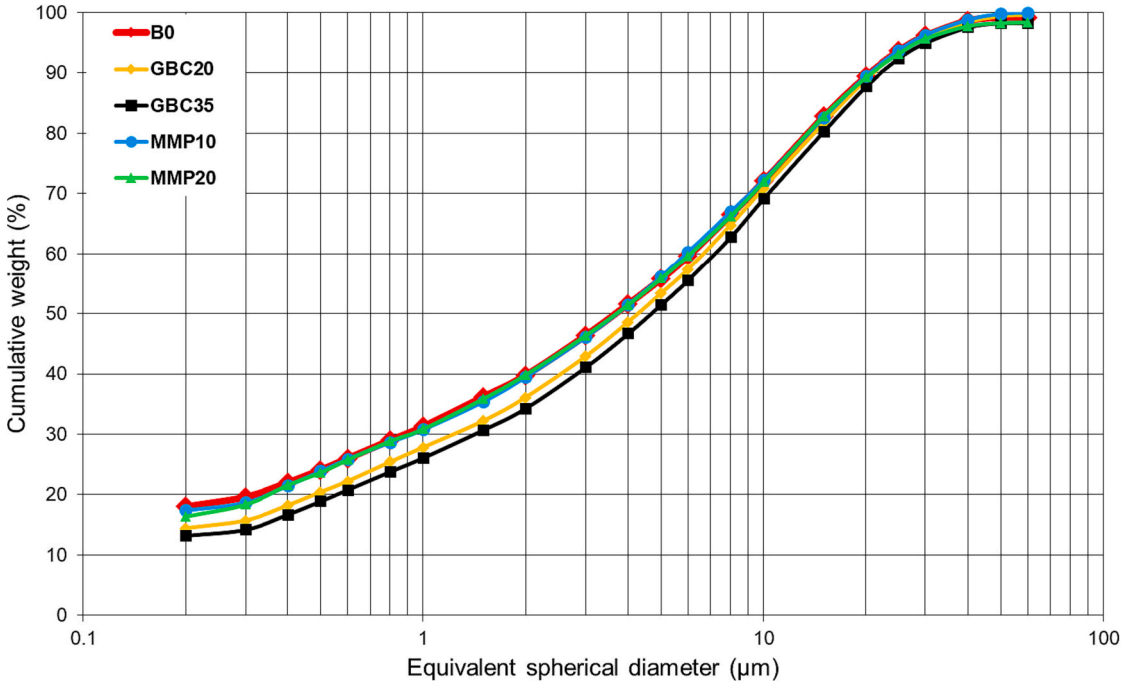

Fig. 5. Particle size distribution of batches B0, GBC20, GBC35, MMP10, MMP20.

Table 6
Resume table of technological properties of the finished products at the maximum densification temperature: LS = linear firing shrinkage (cm/m), WA = water absorption (wt%), BD = bulk density (g/cm^3), OP = open porosity (% vol.).

Property at T_{md}	B0 1200 °C		MMP10 1180 °C		MMP20 1160 °C		GBC20 1220 °C		GBC35 1220 °C	
	mean	std.dev.	mean	std.dev.	mean	std.dev.	mean	std.dev.	mean	std.dev.
LS	5.25	0.00	5.31	0.11	5.49	0.10	6.48	0.06	7.24	0.03
WA	0.10	0.07	0.17	0.11	0.46	0.33	0.08	0.06	0.20	0.09
BD	2.398	0.004	2.419	0.014	2.414	0.003	2.390	0.022	2.396	0.016
OP	0.24	0.17	0.40	0.28	1.12	0.80	0.20	0.13	0.47	0.20

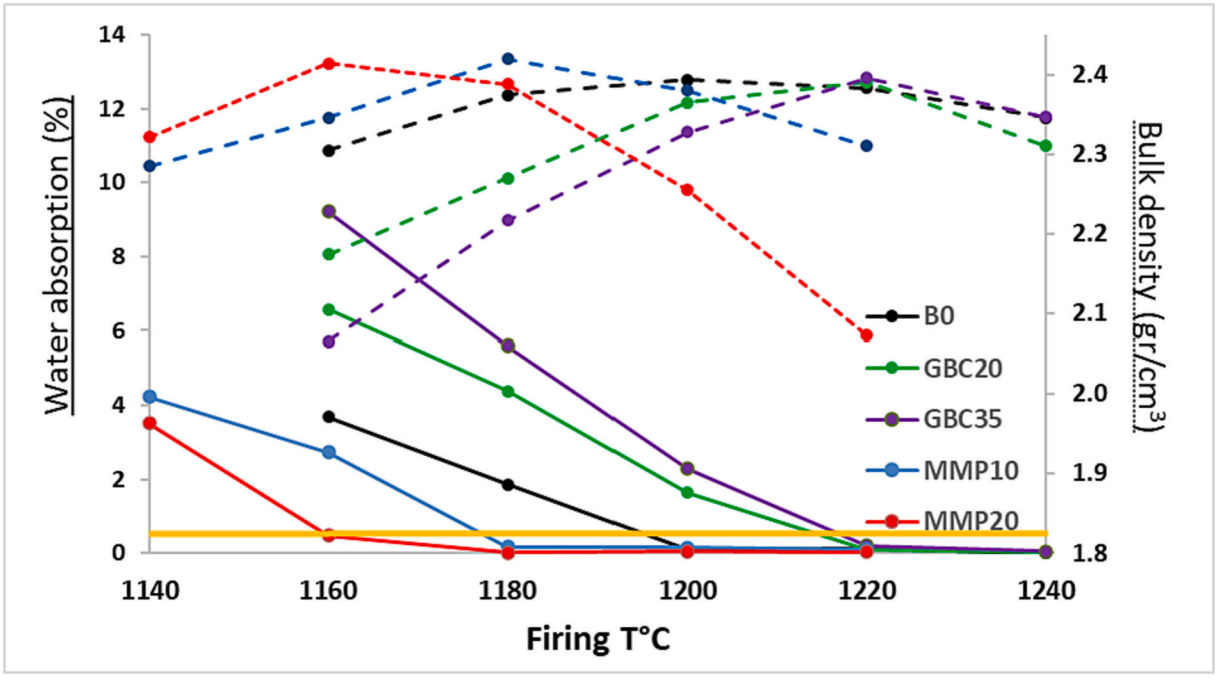

Fig. 6. Gresification curves: water absorption (continuous lines) and bulk density (dashed lines) at the firing Tmax for the various batches. Standard deviations within the symbol size. Red line corresponding to 0.5 wt% of water absorption. (For interpretation of the references to color in this figure legend, the reader is referred to the web version of this article.)

phases, such as quartz for GBC. The bodies fired at the different temperatures were characterized from colorimetric point of view. The data relative to the CIElab coordinate are reported in Table 7, while the picture of the bodied fired at the maximum densification temperature are reported in Fig. 7.

The main changes in the colorimetric coordinates concern the L^* and a^* parameters: all the iron-bearing bodies turned a darker and reddish color (see Fig. 7). In fact, starting from L^* 74.6 of the benchmark, this value decrease to 57 and 50 and to 60 and 47 for the two bodies produced with the addition of GBC and MMP, respectively (Table 7). The a^* parameter scales linearly with increasing the iron content of the batch, passing to 2.8 of B0, to 3.6 and 4.19 for GBC 10 and GCB35, respectively. The increase is even more marked considering the MMP samples, showing values around 9 for sample at the maximum densification temperature. Moreover, an increasing in the b* parameter in MMP bodies can be observed, resulting in more yellow contribution to the final color of these tiles. The color changes indicated from the lowering of L* and increasing of a* and b* can be related with the variation of iron content.

3.8. Phase composition of products fired at the gresification temperature

To unravel the reactions occurred during firing, quantitative phase analyses were carried out. Since detailed kinetic considerations are beyond the aim of this work, only the samples fired at the gresification temperature were analyzed (Table 8).

The main phases in all samples are those generally found in porcelain stoneware tiles: quartz, feldspars and mullite dispersed in prevailing amorphous matrix. The quartz derives from grain not reacted of the initial batch, while mullite is a neoformation phase deriving from high

Table 7
CIE-Lab parameters L^*, a^*, b^* and ΔE^* of the porcelain stoneware batches fired at different temperatures.

sample	T (°C)	1140 °C	1160 °C	1180 °C	1200 °C	1220 °C	1240 °C
B0	L^*		77.93 ± 0.03	74.63 ± 0.03	74.64 ± 0.02	71.40 ± 0.02	71.93 ± 0.02
	a^*		3.50 ± 0.01	2.8 ± 0.016	2.87 ± 0.01	2.50 ± 0.03	2.06 ± 0.02
	b^*		12.75 ± 0.02	12.41 ± 0.03	12.56 ± 0.03	12.57 ± 0.03	12.94 ± 0.03
	ΔE^*		3.36	0.17	0	3.26	2.85
GBC20	L^*		68.80 ± 0.04	63.28 ± 0.02	61.16 ± 0.02	56.89 ± 0.02	59.06 ± 0.02
	a^*		6.12 ± 0.02	5.50 ± 0.02	4.80 ± 0.03	3.60 ± 0.02	2.71 ± 0.04
	b^*		11.27 ± 0.02	11.19 ± 0.03	10.59 ± 0.02	10.49 ± 0.04	11.05 ± 0.03
	ΔE^*		6.81	11.74	13.76	17.89	15.65
GBC35	L^*		64.93 ± 0.02	58.55 ± 0.02	56.54 ± 0.02	50.50 ± 0.02	50.33 ± 0.02
	a^*		7.64 ± 0.02	6.17 ± 0.03	5.64 ± 0.02	4.19 ± 0.02	3.42 ± 0.02
	b^*		11.93 ± 0.04	10.77 ± 0.03	10.48 ± 0.03	9.77 ± 0.03	9.65 ± 0.03
	ΔE^*		10.84	16.52	18.43	24.34	24.49
MMP10	L^*	66.13 ± 0.02	60.51 ± 0.01	57.39 ± 0.01	57.01 ± 0.02	57.73 ± 0.02	
	a^*	9.13 ± 0.03	6.91 ± 0.02	5.90 ± 0.03	5.51 ± 0.02	5.10 ± 0.02	
	b^*	19.55 ± 0.04	16.56 ± 0.04	15.62 ± 0.03	15.47 ± 0.02	15.41 ± 0.02	
	ΔE^*	12.67	15.23	17.78	18.06	17.29	
MMP20	L^*	50.87 ± 0.02	47.86 ± 0.01	46.82 ± 0.02	46.62 ± 0.02	49.00 ± 0.02	
	a^*	11.28 ± 0.04	9.02 ± 0.02	8.35 ± 0.02	8.30 ± 0.03	7.92 ± 0.03	
	b^*	18.35 ± 0.05	15.29 ± 0.04	14.42 ± 0.05	15.39 ± 0.05	16.13 ± 0.07	
	ΔE^*	25.87	27.61	28.42	28.68	26.38	

Fig. 7. Fired samples: comparison among the color of benchmark and sample with Fe bearing clays.

Table 8
Quantitative phase analyses obtained on samples at gresification temperature.

Sample	B0	GBC20	GBC35	MMP10	MMP20
T_{md}	1200 °C	1220 °C	1220 °C	1180 °C	1160 °C
Phase	wt%	wt%	wt%	wt%	wt%
quartz	21.9 (0.3)	25.6 (0.3)	28.4(0.3)	23.3(0.3)	21.8(0.3)
mullite	8.2 (0.2)	7.5 (0.2)	6.9 (0.3)	6.9 (0.3)	3.5 (0.2)
plagioclase	9.2 (0.5)	5.0 (0.5)	5.3 (0.5)	16.7 (0.5)	21.0 (0.5)
pyroxene		2.1 (0.2)	1.6 (0.2)	2.3 (0.2)	2.3 (0.2)
Hematite		0.2 (0.1)	0.3 (0.1)		0.3 (0.1)
Spinel					0.7 (0.1)
Amorphous	60.7 (0.5)	59.6 (0.5)	57.5 (0.6)	50.8 (0.6)	50.4 (0.6)

Rutile and cristobalite are present but present in amount < 0.1 wt.

temperature treatment. The degree of vitrification, desumed from the amount of amorphous phase, is higher in the benchmark and the bodies with the German red clay (57–61%) than in bodies with MMP that contain around 50%. From the data reported in Table 8 it is possible to see that GBC20 an GBC35 show the greatest amount of residual quartz (~26 and ~ 28%, respectively, against 22–23% of the benchmark and the MMP-bearing samples). As a residual phase, it is likely inherited from raw batches, as those with the addition of GBC have a higher amount of quartz. On the contrary, plagioclase contents are higher for the MMP samples: this can be attributed to the lower firing temperatures reached for these batches (1160–1180 °C). Such temperatures allowed the persistence of much more plagioclase with respect to the other samples fired at 1200–1220 °C. The chance of anorthite formation during firing has been ruled out, given that the difference in CaO between the batches is minimal and the structural parameters of plagioclase in the fired products are substantially the same as the starting albite. Mullite contents is in the 7–8% range for all the investigated samples, with the exclusion of MMP20 that has about 3%.

Minor phases were found in all the batches, e.g., iron-bearing phases (pyroxene and hematite) in clear relation with the Fe_2O_3 contents of the batches. Cristobalite and rutile were always found, but in amount around the detection limit of the technique (0.1 wt%), so it has not been possible to exactly quantify these phases. The presence of spinel was evidenced only for sample MMP20, likely because this batch is the richest in MgO.

4. Conclusions

As the iron content in porcelain stoneware bodies is increasing in many countries, as a result of the use of local raw materials to replace traditional ball clays, it is important to understand the effect of Fe on the technological properties. This study took into consideration different red clays, trying first of all to determine in what form the iron is in the raw materials. It's worth noting that the main mineralogical components of the Italian red clays (i.e. coming from Val Rossenna varicolored shales and Monte Piano Formation) are illite and I/Sm mixed layer phyllosilicates. Chlorite is present in very low amounts contrarily to what generally reported for this kind of materials. The high amount of iron of the clays is due to the presence of oxides and hydroxides (crystalline and amorphous), but even to the presence of high amount of Fe ions in the clay minerals structure. The German red clay, used as mean of comparison, resulted to be richer in kaolinite and, especially in quartz that makes the raw material more refractory.

The results of process simulation at laboratory scale indicate that the partial substitution of the highly plastic clays generally employed in the industrial production of porcelain stoneware is possible without severe technological bottlenecks. However, the grindability worsened when using 20–35% low plasticity red clays (GBC), while the rheological behavior of the slip worsened in the presence of 10–20% highly plastic red clays, rich in I—S mixed layers (MMP). Both drawbacks can be easily overcome by increasing the milling time and the amount of deflocculant, respectively. Powder compressibility is also influenced by particle size distribution and mineralogical composition: it improves with MMP (more expandable clay minerals) and worsens with GBC (more kaolinite and coarser grain size).

Notwithstanding the batch chemical composition has been maintained as constant as possible in terms of silica and alkalis, the use of red clays heavily affected the firing behavior. MMP induced a lowering of gresification temperature with respect to the benchmark (20–40 °C) while GBC led to slightly higher gresification temperature but also reduced the dimensional stability. The firing behavior of Fe-enriched bodies is not as expected, and some evidence has emerged about the iron phases and the stability of feldspar, quartz and mullite. In this regard, a study of the role of iron in the vitrification path and sintering kinetics is necessary, which will be the subject of another article.

Nonetheless, it has always been possible to obtain products compliant with porcelain stoneware standards. This can pave the way toward the exploitation of local resources in order to mitigate the supply risk and limit the economic and environmental costs linked to the import of raw materials over long distances. The strongest limitation observed in the technological properties of the final product is obviously the color, given that in the present case study the use of red clay was accentuated, bringing the Fe_2O_3 content of the batch from 0.66% of the benchmark up to 2%.

CRediT authorship contribution statement

Riccardo Fantini: Investigation, Methodology, Writing – original draft. **Sonia Conte:** Conceptualization, Data curation, Investigation, Writing – original draft, Validation. **Alessandro F. Gualtieri:** Conceptualization, Data curation, Supervision, Validation, Writing – review & editing. **Michele Dondi:** Conceptualization, Project administration, Supervision, Validation. **Francesco Colombo:** Investigation. **Mattia Sisti:** Investigation. **Chiara Molinari:** Investigation. **Chiara Zanelli:** Data curation, Investigation, Supervision, Writing – review & editing. **Rossella Arletti:** Conceptualization, Project administration, Supervision, Validation, Writing – original draft, Writing – review & editing.

Declaration of competing interest

The authors declare that they have no known competing financial interests or personal relationships that could have appeared to influence

the work reported in this paper.

Data availability

Data will be made available on request.

Acknowledgements

Vignudini e Pinelli s.r.l, Ruggi s.r.l. and Stephan Schmidt Group are acknowledged for providing the clay sample.

Appendix A. Supplementary Data

Supplementary data to this article can be found online at https://doi.org/10.1016/j.clay.2024.107291.

References

ACIMAC, 2022. World Production And Consumption Of Ceramic Tiles 10th Edition Year 2022 Trend 2012–2021.

Bertolani, M., Biondini, R., Giliberti, T., Loschi, A.G., Rabitti, D., 1982. Caratteristiche chimiche e mineralogiche di campioni di argille per ceramica dell'area Sassolese. La Ceramica 35, 16–33.

Bettelli, G., Bonazzi, U., Bettelli, P., Panini, F., 1989a. Schema introduttivo alla geologia delle Epiliguridi dell'Appennino modenese e delle aree limitrofe. Memorie Della Società Geologica Italiana 39, 215–244.

Bettelli, G., Bonazzi, U., Panini, F., 1989b. Schema introduttivo alla geologia delle Liguridi dell'Appennino modenese e delle aree limitrofe. Memorie Della Società Geologica Italiana 39, 91–126.

Bettelli, G., Panini, F., Pizziolo, M., 2002. NOTE ILLUSTRATIVE della CARTA GEOLOGICA. D'ITALIA alla scala 1, 50.000.

Bornhöft, E., Kleeberg, K., 2012. Feldspatrohstoff. In: Geol. Jb. Börner, A., Bornhöft, E., Häfner, F., Hug-Diegel, N., Kleeberg, K., Mandl, J., Schäfer, I. (Eds.), Steine-Und Erden-Rohstoffe in Der Bundesrepublik Deutschland, pp. 219–230.

Capelli, R., Bertolani, M., 1991. Caratterizzazione delle materie prime argillose del bacino estrattivo Secchia-Dorgola, in comune di Carpineti (prov. RE). Ceramurgia 21, 3–14.

Conte, S., Buonamico, D., Magni, T., Arletti, R., Dondi, M., Guarini, G., Zanelli, C., 2022. Recycling of bottom ash from biomass combustion in porcelain stoneware tiles: Effects on technological properties, phase evolution and microstructure. J. Eur. Ceram. Soc. 42, 5153–5163. https://doi.org/10.1016/j.jeurceramsoc.2022.05.014.

Conte, S., Molinari, C., Ardit, M., Cruciani, G., Dondi, M., Zanelli, C., 2023. Porcelain versus Porcelain Stoneware: so Close, so different. Sintering Kinetics, Phase Evolution, and Vitrification Paths. Materials 16, 171. https://doi.org/10.3390/ma16010171.

Degen, T., Sadki, M., Bron, E., König, U., Nénert, G., 2014. The HighScore suite. Powder Diffract. 29 https://doi.org/10.1017/S0885715614000840.

Doebelin, N., Kleeberg, R., 2015. Profex: a graphical user interface for the Rietveld refinement program BGMN. J. Appl. Crystallogr. 48, 1573–1580. https://doi.org/10.1107/S1600576715014685.

Dondi, M., 1999. Clay materials for ceramic tiles from the Sassuolo District (Northern Apennines, Italy). Geology, composition and technological properties. Appl. Clay Sci. 15, 337–366. https://doi.org/10.1016/S0169-1317(99)00027-7.

Dondi, M., Guarini, G., Raimondo, M., Salucci, F., 2003. Influence of Mineralogy and Particle Size on the Technological Properties of Ball Clays for Porcelainized Stoneware Tiles 20.

Dondi, M., Guarini, G., Conte, S., Molinari, C., Soldati, R., Guarini, C., 2019. Deposits, composition and technological behavior of fluxes for ceramic tiles. Periodico di Mineralogia 88. https://doi.org/10.2451/2019PM861.

Dondi, M., García-Ten, J., Rambaldi, E., Zanelli, C., Vicent-Cabedo, M., 2021. Resource efficiency versus market trends in the ceramic tile industry: effect on the supply chain in Italy and Spain. Resour. Conserv. Recycl. 168, 105271 https://doi.org/10.1016/j.resconrec.2020.105271.

Fahimnia, B., Sarkis, J., Davarzani, H., 2015. Green supply chain management: a review and bibliometric analysis. Int. J. Prod. Econ. 162, 101–114. https://doi.org/10.1016/j.ijpe.2015.01.003.

Fiederling-Kapteinat, H.-G., 2004. The Ukrainian clay mining industry and its effect on the European ceramic raw materials market, part 1. InterCeram: Intern. Ceramic Rev. 53, 396–399.

Fiederling-Kapteinat, H.-G., 2005. The Ukrainian clay mining industry and its effect on the European ceramic raw materials market part 2. InterCeram: Intern. Ceramic Rev. 54, 4–8.

Fiori, C., Guarini, G., 1990. Italian red clays for stoneware tile production: statistical study of the mineralogical composition. Ind. Ceram. 10, 151–157.

Franzini, M., Leoni, L., Saitta, M., 1975. Revisione di una metodologia analitica per fluorescenza-X, basata sulla correzione completa degli effetti di matrice. Rend. Soc. Ital. Mineral. Petrol. 31, 365–378.

Galos, K., 2011a. Composition and ceramic properties of ball clays for porcelain stoneware tiles manufacture in Poland. Appl. Clay Sci. 51, 74–85. https://doi.org/10.1016/j.clay.2010.11.004.

Galos, K., 2011b. Influence of mineralogical composition of applied ball clays on properties of porcelain tiles. Ceram. Int. 37, 851–861. https://doi.org/10.1016/j.ceramint.2010.10.014.

Gualtieri, A., 2000. Accuracy of XRPD QPA using the combined Rietveld–RIR method. J. Appl. Crystallogr. 33 https://doi.org/10.1107/S002188989901643X.

Gualtieri, A.F., Gatta, G.D., Arletti, R., Artioli, G., Ballirano, P., Cruciani, G., Guagliardi, A., Malferrari, D., Masciocchi, N., Scardi, P., 2019. Quantitative phase analysis using the Rietveld method: towards a procedure for checking the reliability and quality of the results. Periodico di Mineralogia 88. https://doi.org/10.2451/2019PM870.

Leoni, L., Saitta, M., 1976. X-ray fluorescence analysis of 29 trace elements in rock and mineral standards. Rend. Soc. Ital. Mineral. Petrol. 32, 497–519.

Moore, D.M., Reynolds Jr., R.C., 1989. X-ray Diffraction and the Identification and Analysis of Clay Minerals.

Petrick, K., Diedel, R., Peuker, M., Dieterle, M., Kuch, P., Kaden, R., Krolla-Sidenstein, P., Schuhmann, R., Emmerich, K., 2011. Character and Amount of I-S Mixed-layer Minerals and Physicalchemical Parameters of two Ceramic Clays from Westerwald, Germany: Implications for Processing Properties. Clay Clay Miner. 59, 58–74. https://doi.org/10.1346/CCMN.2011.0590108.

Polidori, E., Gori, U., 2005. Classificazione dei terreni argillosi. Giornale di Geologia Applicata 2, 249–254.

Timillini, G., Fregni, A., Rinaldi, C., 1999. Use of local raw materials for the manufacture of ceramic floor and wall tile by companies located in the ceramic district of Sassuolo (Italy): environmental aspects. Ceramica Acta 11, 21–31.

Vignudini, R., Venturi, V., 1996. La cava di Morano (Prignano - Modena) e la sua argilla. Ceramica Inf 360, 158–163.

Zanelli, C., Iglesias, C., Domínguez, E., Gardini, D., Raimondo, M., Guarini, G., Dondi, M., 2015. Mineralogical composition and particle size distribution as a key to understand the technological properties of Ukrainian ball clays. Appl. Clay Sci. 108, 102–110. https://doi.org/10.1016/j.clay.2015.02.005.

Zanelli, C., Soldati, R., Conte, S., Guarini, G., Ismail, A.I.M., El-Maghraby, M.S., Cazzaniga, A., Dondi, M., 2018. Technological behavior of porcelain stoneware bodies with Egyptian syenites. Int. J. Appl. Ceram. Technol. 16, 574–584. https://doi.org/10.1111/ijac.13102.

Zanelli, C., Domínguez, E., Iglesias, C., Conte, S., Molinari, C., Soldati, R., Guarini, G., Dondi, M., 2019. Recycling of residual boron muds into ceramic tiles. Boletín de la Sociedad Española de Cerámica y Vidrio 58, 199–210. https://doi.org/10.1016/j.bsecv.2019.01.002.

Zanelli, C., Conte, S., Molinari, C., Soldati, R., Dondi, M., 2021. Waste recycling in ceramic tiles: a technological outlook. Resour. Conserv. Recycl. 168, 105289 https://doi.org/10.1016/j.resconrec.2020.105289.